Received Date : 04-Oct-2016

Revised Date : 17-Feb-2017

Accepted Date : 21-Feb-2017

Article type : Research Letter

Investigating the effect of available redox protein ratios for the conversion of a steroid by a myxobacterial CYP260A1

Yogan Khatri[1Ψ], Alexander Schifrin[1], and Rita Bernhardt[1]*

[1]Saarland University, Institute of Biochemistry, Campus B2.2, 66123, Saarbrücken, Germany.

***Corresponding author:**

Prof. Dr. Rita Bernhardt

Institute of Biochemistry,

Saarland University,

Campus B 2.2,

D-66123 Saarbruecken, Germany.

This is the author manuscript accepted for publication and has undergone full peer review but has not been through the copyediting, typesetting, pagination and proofreading process, which may lead to differences between this version and the Version of Record. Please cite this article as doi: 10.xxxx/feb2.12619

Phone: +49 681 302 4241

Fax: +49 681 302 4739

E.mail: ritabern@mx.uni-saarland.de

[Ψ] Current address

Yogan Khatri

Life Sciences Institute

University of Michigan

Ann Arbor, Michigan 48109, United States

Highlights:

- CYP260A1 converts 11-deoxycorticosterone, the Δ4-C21 steroid, into 1α-hydroxy-11-deoxycorticosterone as a major product.
- The available redox protein ratios during the conversion of 11-deoxycorticosterone by CYP260A1 affect the catalytic activity and product pattern.
- Higher redox protein availability supported the further conversion of 1α-hydroxy-11-deoxycorticosterone into the dihydroxylated product 1α-, 14α-dihydroxy-11-deoxycorticosterone and C1-C2-ene-11-deoxycorticosterone .
- 1α-, 14α-dihydroxy-11-deoxycorticosterone is a novel steroidal derivative.

Abstract

Since cytochromes P450 are external monooxygenases, available surrogate redox partners have been used to reconstitute the P450 activity. However, the effect of various ratios of P450s and the redox proteins have not been extensively studied so far, although different combinations of the redox partners have shown variations in substrate conversion. To address this issue, CYP260A1 was reconstituted with various ratios of adrenodoxin and adrenodoxin reductase to convert 11-deoxycorticosterone, and the products were characterized by NMR. We show the effect of the available redox protein ratios not only on the P450 catalytic activity but also on the product pattern.

Key words:

P450, redox-protein-ratios, steroid

Abbreviations

AdR, Adrenodoxin reductase; Adx, Adrenodoxin; DOC, deoxycorticosterone

Introduction

Cytochromes P450 (P450s), the heme-containing monoxygenase enzymes, are able to catalyze a variety of chemical reactions including C-H functionalization, aromatic hydroxylation, dealkylation, C–C lyase activity, decarboxylation, nitration and carbene transfer [1, 2]. P450s are also involved in the biosynthesis of natural products [3]. They require electrons for their activity, which can be donated by autologous or heterologous redox partners via an electron transfer chain [4]. However, the requirement of efficient redox partners to deliver electrons from NADH or NADPH to a P450 is the bottleneck for its application [5].

The identification of functional autologous or heterologous redox partners for orphan microbial P450s is complicated, because the P450s and potential redox partners are not always found in the same gene cluster [6]. However, surrogate redox partners are often employed to reconstitute catalytic activities for such novel P450s. Several different redox systems, like putidaredoxin reductase (PdR) – putidaredoxin (Pdx) from *Pseudomonas putida,* adrenodoxin reductase homolog 1 (Arh) – endogenous ferredoxin component (etp1) from *Schizosaccharomyces pombe* [7], ferredoxin reductase (FdR) – ferredoxin (Fdx) from *E. coli* [8], ferredoxin reductase (FdR) – flavodoxin (*yku*N/ *yku*P) from *Bacilus subtilis* [9], adrenodoxin reductase (AdR) – adrenodoxin (Adx) from bovine adrenals [10], the reductase domain of CYP102A1 (BMR) [9, 11], the FMN- and Fe/S-containing domain of p450RhF from *Rhodococcus* sp. [12], a phthalate family oxygenase reductase (PFOR) from *Pseudomonas putida* KT24440 [13], along with the chimeric systems of SynFdx (Fd) from *Synechocystis* and the ferredoxin $NADP^+$ reductase (FNR) from *Chlamydomonas reinhardtii* [14] and Adx-FpR from *E. coli* [15] as well as the commercially available spinach ferredoxin (Fdx) and ferredoxin reductase (FdR) [16, 17] have been used in different ratios to reconstitute the activity of various P450s. However, the ratios of P450 and the redox partners used for the substrate conversions were not consistent in the different studies. In some studies more than a 10-fold [9, 18-20], a 20-fold [21, 22], a 50-80 fold [23-25] or even more than a 200-fold [26, 27] higher ratio of Fdx compared with the P450 was employed for the *in vitro* conversion of the related substrate. In all these studies, the main aim of employing the various ratios was to make the P450 functional, but the effect of different ratios of the redox partners was not studied. Nevertheless, it has been shown that the use of surrogate redox systems for a

novel P450 not only showed variations in the substrate conversion [14, 15, 28-30] but also displayed different product selectivities [31]. In addition, the use of non-physiological substrates containing multiple oxidation sites to be attacked by a P450, generally resulted in different oxidized products depending on the reaction conditions and incubation time, in which the earlier product(s) might serve as a substrate for further conversions [32, 33]. Such multi-step or sequential oxidations of a substrate by a P450 results in either a distributive, (obtaining multi-hydroxylated products at once as shown e.g. for CYP19 [34, 35]) or a processive (step-wise sequential reactions as observed for the conversion of nitrosamines to aldehydes and then carboxylic acids by CYP2A6 [33, 36]) product distribution.

While using a non-physiological substrate for a P450 or a mutated variant of a specific P450, in some of the cases the product patterns that are observed in an *in vitro* reaction do not replicate in the *in vivo* conversion [37]. In general, the amounts of the redox partners being present during the co-expression of P450 and redox partners in a whole-cell system are not comparable to the amounts of the redox proteins in the *in vitro* reaction. Therefore, this study attempted to investigate this issue in more detail. In order to understand the effect of the redox protein ratio of Adx and AdR on the P450-dependent reaction, different amounts of the redox proteins were used for the conversion of 11-deoxycorticosterone (DOC) by CYP260A1. We studied the consequences on the conversion of DOC and its product selectivity during the *in vitro* reaction and the *E. coli* based whole-cell system. The obtained main products were purified and characterized by liquid chromatography mass spectrometry (LC-MS) and nuclear magnetic resonance 1D- and 2D-NMR analysis.

Materials and methods

Molecular cloning, expression and purification of CYP260A1

The heterologous expression, purification and characterization of CYP260A1 was performed as described elsewhere [10]. The mammalian adrenodoxin reductase, AdR, and truncated adrenodoxin, Adx_{4-108}, were expressed and purified as described [38, 39].

In vitro enzyme activity assay

The conversion of DOC by CYP260A1 was carried out with the heterologous electron partners. The *in vitro* reconstitution assay to determine the steady-state conversion of DOC (100 μM) was performed in a final volume of 250 μl containing a mixture of CYP260A1 (0.5 μM), Adx (5 μM), AdR (1.5 μM) (CYP260A1: Adx: AdR of 1: 10: 3), and substrate (100 μM)

in 20 mM potassium phosphate buffer (pH 7.4). The reaction was started by adding NADPH (500 µM) and incubating for 20 min at 30°C, and stopped by the addition of chloroform (500 µl). The sample was mixed vigorously, and the organic phase was extracted twice with chloroform. The pooled samples were dried and analyzed by HPLC as described [10]. The time-dependent conversion was done by increasing the incubation time (5 - 100 min). The NADPH dependent conversion of the substrate was done using 100 µM to 4 mM freshly prepared NADPH under the same condition as explained. The reaction was done in the absence or presence of a NADPH regeneration system when needed. The NADPH-regenerating system consists of glucose 6-phosphate (5 mM), glucose 6-phosphate dehydrogenase (1 U), and $MgCl_2$ (1 mM). Protein ratios of CYP260A1: Adx: AdR of (1: 1: 1, 1: 2: 0.5, 1: 1: 5, 3: 2.5: 1, 8: 3: 1, 1: 5: 1, 1: 5: 3, 1: 5: 5, 1: 10: 1, 1: 10: 2, 1: 10: 3, 1: 10: 5, 1: 10: 7, 1: 10: 10, 1: 20: 1, 1: 20: 3, 1: 20: 5, 1: 20: 7, 1: 20: 10, 1: 10: 15, or 1: 20: 20) was used. The related protein concentrations are used as mentioned in Table 1 and Figure 2.

To investigate the effect of radical scavengers on the catalytic rate, the in vitro conversions were performed with the addition of ascorbate (20 mM), catalase (20 U) and superoxide-dismutase (SOD) (3 U), individually as well as in combination. To determine whether hydrogen peroxide (H_2O_2) could be applied to reconstitute the activity of CYP260A1, H_2O_2 was used in a final concentration of 50 µM. The reactions were stopped, extracted and analyzed as described below. All the experiments were performed by using the same batch of purified proteins.

Whole-cell biotransformation using resting cells

The whole-cell biotransformation assay was performed in *E. coli* C43(DE3) cells. The cells were transformed with two plasmids, one for the CYP260A1 and the other one for the redox partners AdR and $Adx_{4\text{-}108}$ as described [15]. The conversion of DOC by the resting cells expressing the redox partners and CYP260A1 was performed as described [10].

Detection and analysis of substrate conversion by CYP260A1

The analysis of the DOC conversion in HPLC and LC-MS was performed as described [10]. Briefly, the *in vitro* and the *in vivo* conversions of the steroids were analyzed by reversed phase HPLC. After evaporation of the organic (chloroform) phase, the steroids were resuspended in 80% acetonitrile and separated on a Jasco reversed phase HPLC system (Tokyo, Japan) composed of an auto sampler AS-2050 plus, pump PU-2080, gradient mixer LG-2080-02 and an UV-detector UV-2075. A reversed phase column (Nucleodur R100-5

C18ec, particle size 3 µm, length 125 mm, internal diameter 4 mm, Macherey-Nagel) was used to separate the substrate (DOC) from its products (1α-,14α-dihydroxy-11-DOC, 1α-hydroxy-11-DOC, or C1-C2-ene-11-DOC). The separation of the steroids was done by a gradient elution of acetonitrile 10-100% from 0-10 min and was monitored at 240 nm. The column temperature was kept constant at 40°C with a peltier oven. 20 µl of the samples were injected for analysis. The peaks were identified by using the ChromPass software (V.1.7.403.1, Jasco) and the conversion rate (nmol total product per nmol CYP260A1 per min) was calculated. DOC, 1α-hydroxyl-11-DOC and C1-C2-ene-11-DOC (NMR-characterized) were used as standards to identify the retention time (RT) of the peaks on HPLC.

Binding study of DOC and 1α-hydroxy-11-DOC

Spin-state shifts upon substrate binding were assayed at 25°C under aerobic conditions using an UV–visible scanning spectrophotometer (UV-2101PC, Shimadzu, Japan) equipped with two tandem quartz cuvettes (Hellma, Müllheim, Germany) as described [10, 30]. One chamber of each cuvette contained 1.12 µM CYP260A1 in 800 µl of 10 mM potassium phosphate buffer, pH 7.4, whereas the second chamber contained buffer alone. The titration of the substrates (DOC and 1α-hydroxyl-11-DOC dissolved in DMSO) was done by adding small (< 1 µl) aliquots of an appropriate stock of the substrate into the P450 containing chamber of the sample cuvette. An equal amount of the substrate was also added into the buffer containing chamber of the reference cuvette, and spectral changes between 200 - 700 nm were recorded. The overlaid difference spectra from 350 - 500 nm produced by subtraction of the spectrum for ligand-free CYP260A1 from the successive spectra for substrate-bound species accumulated during the titration of testosterone and androstenedione were obtained.

The dissociation constants (K_d) for CYP260A1 with DOC and 1α-hydroxylated DOC were calculated by fitting the peak-to-trough difference against substrate concentration to a nonlinear tight binding quadratic equation [40]. The relevant equation is: $\Delta A = (A_{max}/ 2[E]) \{(K_d + [E] + [S]) - \{(K_d + [E] + [S])^2 – 4 [E] [S]\}^{1/2}\}$, where ΔA represents the observed peak-to-trough absorbance difference at each substrate addition, A_{max} is the maximum absorbance difference at substrate saturation, [E] is the total enzyme (CYP260A1) concentration and [S] is the substrate concentration. The data fitting was performed using Origin 8.1G software. All titrations were done for three times and the K_d values reported are the mean for the three sets of the experimental data.

NMR characterization of the CYP260A1 product

The fractions of the purified product were pooled and dried in a rotary evaporator. The residue was dissolved in $CDCl_3$ for NMR analysis. NMR (^1H and ^{13}C NMR) data were recorded with a Bruker DRX (Rheinstetten, Germany) 500 NMR spectrometer at 300 K at the NMR spectroscopy facility (Institut für Pharmazeutische Biologie, Universität des Saarlandes). The chemical shifts were relative to $CHCl_3$ at δ 7.24 (^1H NMR) or $CDCl_3$ at δ 77.00 (^{13}C NMR) using the standard δ notation in parts per million (ppm). The 1D NMR (^1H and ^{13}C NMR, DEPT135) and the 2D NMR spectra (gs-HH-COSY, gs-NOESY, gs-HSQCED, and gs-HMBC) was recorded using Bruker pulse program library.

Results and discussion

Determination of *in vitro* steady-state conditions for DOC conversion by CYP260A1

In order to investigate the effect of redox protein ratios for the conversion of DOC by CYP260A1, we employed the bovine redox partners $Adx_{(4\text{-}108)}$ and AdR, which have been identified as the most efficient redox partners for several myxobacterial [15, 30, 41] and bacillus [28, 42] P450s, as well as the CYP260 family from *Sorangium cellulosum* So ce56 [10, 43]. Adx is one of the most thoroughly studied redox proteins to date [44, 45]. Furthermore, very recently we have shown that an *E. coli* based whole-cell system with CYP260A1, co-expressing the bovine ferredoxin and an *E. coli* ferredoxin reductase, was able to convert Δ4-C19 steroids [10]. However, the effect of the available redox protein pool on the conversion of steroids has not been studied. In this study, we used DOC, the Δ4 C-21 steroid, as a substrate which is converted into multiple hydroxylated products so that changes in the selectivity can easily be followed.

At first, the time dependent *in vitro* DOC conversion by CYP260A1 at substrate saturation (100 µM) using the ratio of CYP260A1: Adx: AdR of 1: 10: 3 was performed to investigate the steady-state conditions of the conversion (Figure 1. A-B). The LC-MS measurement of the *in vitro* conversion of DOC (peak S with $[M+Z]^+$ = 331.2) showed two main products, peak 4 (~26% with $[M+H]^+$ of 347.2) and peak 6 (~11% with $[M+H]^+$ of 329.2) at retention times (t_R) of 5.28 min and 7.13 min, respectively, as well as 4 side-products corresponding to the peaks 1 (~7% with $[M+Z]^+$ = 363.2), 2 (~7% with $[M+Z]^+$ = 345.2), 3 (~7% with $[M+Z]^+$ = 347.2), and 5 (~7% with $[M+Z]^+$ = 347.2) at t_R of 4.13, 4.41, 5.07, and 6.36 min, respectively (Figure 1.A).

We observed that the conversion was in a steady-state condition up to 40 min (Figure 1.B). In accordance with this, 20 min reaction time was used for the subsequent *in vitro* conversions utilizing the same batch of the purified CYP260A1, Adx and AdR at a ratio of 1: 10: 3 for CYP260A1: Adx: AdR (0.5 µM: 5 µM: 1.5 µM). In order to determine the concentration of NADPH to be used for the steady-state condition, a saturating concentration of DOC (100 µM) was converted using increasing concentrations of NADPH (Figure 1. C), which showed values of K_m and V_{max} of 354 ± 85 µM and 1.67 ± 0.10 min^{-1}, respectively. The K_m value does not mean the kinetic parameter of AdR, but rather represents the concentration of NADPH at which the reaction rate is half of the maximum rate in the coupling reaction by the redox partners and CYP260A1. Afterwards, for the subsequent study of DOC conversion, 500 µM NADPH was used. Moreover, turnover experiments of DOC (100 µM) in the presence and absence of a NADPH regeneration system were performed, and it was observed that the rate is almost the same as in the case of absence of NADPH recycling (1.7 *vs* 1.8 min^{-1}) (Figure 1. D). Therefore, for the subsequent conversion of DOC by CYP260A1, different ratios of CYP260A1 and redox partners were used in the absence of NADPH regeneration.

Conversion of DOC by utilizing different ratios of CYP260A1 and redox proteins

In a first set of experiments we compared the activities of DOC conversion for ratios of P450 : Fdx: FdR, which have been employed in previous studies [46, 47]. At first, an equimolar concentration of P450: Adx: AdR of 1: 1: 1 [46] (Figure 2, entry A), and an increased ratio of ferredoxin and decreased ratio of ferredoxin reductase of 1: 2: 0.5 [47] (Figure 2, entry B), as well as a ratio allowing a higher amount of the reductase compared to the P450 and the ferredoxin of 1: 1: 5 (Figure 2, entry C) were used for the *in vitro* conversion of DOC by CYP260A1. We observed that the conversion consisting of slightly higher molar ratios of Adx compared to CYP260A1 and AdR showed higher turnover (1.23 min^{-1} i.e. nmol total products per nmol CYP260 A1 per min) (Figure 2, entry B) compared with the equimolar ratio of 1: 1: 1 (0.90 min^{-1}) (Figure 2, entry A) and increased AdR ratio of 1: 1: 5 (0.65 min^{-1}) (Figure 2, entry C).

In addition, we also employed the ratios of 3: 2.5: 1 and 8: 3: 1 for CYP260A1: Adx: AdR, displaying a higher molar ratio of P450 compared with the redox partners for DOC conversion. These ratios were used for the *in vitro* conversion of steroidal substrates by mitochondrial cytochromes P-450s using Adx and AdR as redox partners [48]. We observed that the higher ratio of CYP260A1 compared with Adx and AdR did not increase the rate of

DOC conversion, showing a turnover of 0.60 min^{-1} for CYP260A1: Adx: AdR of 3: 2.5: 1 (Figure 2, entry D) and of 0.45 min^{-1} for a ratio of 8: 3: 1 (Figure 2, entry E).

In order to systematically investigate the effect of the redox protein ratios on DOC conversion, three experimental sets consisting of a 5- (Figure 2, entry F-H), 10- (Figure 2, entry I-N) and 20-fold higher molar ratio of Adx (Figure 2, entry O-U) compared with CYP260A1 at increasing ratios of AdR compared with CYP260A1 were used (Table 1). We observed a maximum turnover rate of 2.61 ± 0.10 min^{-1}, 1.96 ± 0.10 min^{-1} and 1.62 min^{-1} for the ratio of CYP260A1: Adx: AdR of 1: 20: 3, 1: 10: 3 and 1: 5: 3, respectively. Interestingly, it was observed that at higher ratios of AdR than 1:3 compared with CYP260A1 a diminished turnover rate for the substrate conversion was observed, which was also true for the ratio that has been used for an earlier study [48] (Figure 2, entry C). In addition, an equal or higher molar ratio of P450 compared to Adx also showed a reduced activity (Figure 2, entries A, D-E). In order to reconstitute the activity of several P450s, different ratios of the P450 and redox partners were also employed in earlier studies. However, a higher concentration of ferredoxin with a lower reductase ratio [47, 49-51] or a higher concentration of P450 compared to Fdx and FdR [52] were used. Very recently, we have observed a higher conversion of epothilone D by the P450 EpoK when using the ratio of 1: 20: 3 compared to 1: 10: 1 for EpoK : Fdx: reductase (either AdR, Arh1 or FNR).

In general, as shown in Figure 2, the highest turnover numbers were obtained with a ratio of CYP260A1: Adx: AdR of 1: 20: 3. It has been shown that a 2-fold higher concentration of adrenodoxin reductase is required for maximal P450scc (CYP11A1) activity in the presence of a relatively high concentration of adrenodoxin (~ 10-fold) [53, 54]. During the steady-state conversion of DOC by CYP260A1, we observed that the presence of higher amounts of Adx showed higher activities (Figure 2). Although the mechanism of interaction of P450s with Adx-AdR is well studied for CYP11A1 and it has been suggested that Adx can make either productive tertiary or quaternary complexes with bovine CYP11A1 [55, 56] and AdR or can shuttle electrons through the formation of Adx or Adx-dimers [57, 58], the detailed mechanism of the interaction of the redox partners with CYP260A1 still needs to be elucidated. However, it can be suggested that at higher amounts of Adx the delivery of electrons becomes faster thus leading to an efficient DOC conversion. In contrast, the increase of the AdR concentration compared to CYP260A1 and Adx in the *in vitro* reaction significantly dropped the rate of DOC conversion (Figure 2), which might be the result of a decreased concentration of free Adx protein that is required for shuttling the electrons from

the AdR to CYP260A1. In addition, the higher rate of non-specific NADPH oxidation by the increased reductase concentration could also account for the lower conversion.

Effect of redox protein ratios on the product pattern of the DOC conversion by CYP260A1

Most interestingly, the *in vitro* product pattern of DOC conversion using different ratios of P450 and the redox proteins changed significantly when using various ratios of the proteins. Although the same 6 product peaks were observed as under the steady-state conditions (Figure 1. B), their relationship changed considerably, especially for the major product peaks 4 (t_R = 5.28 min, *Δm/z* of +16) and 6 (t_R = 7.13 min, *Δm/z* of +2) as well as the minor product peak 1 (t_R = 4.13 min, *Δm/z* of +32) (Figure 3.A, Supplemental Figure S1). When the ratio of CYP260A1: Adx: AdR was 1: 5: 3, peak 6 was the highest followed by peak 4 (Figure 3.A). In order to study the effect of the incubation time of the reaction, time dependent DOC conversion in the presence and absence of a NADPH recycling system was performed. However, there was no change in the product pattern (Supplementary Figure S1).

When increasing the amount of the redox proteins relative to CYP260A1 to a ratio of CYP260A1: Adx: AdR of 1: 10: 3 or 1: 20: 3, product peak 6 was gradually decreased and peak 4 (t_R = 5.28 min) was increased (Figure 3. A), respectively. The time dependent product formation observed by using CYP: Adx: AdR of 1: 10: 3 in the absence of a NADPH recycling system did not show any differences in the product pattern compared with the 30 min to 2 hr reaction time (Supplemental Figure S2).

In a subsequent experiment, when the time dependent conversion of DOC was performed in the presence of a NADPH recycling system and the highest ratio of the redox proteins (CYP260A1: Adx: AdR of 1: 20: 3), the highest yield of the product peak 1 (t_R = 4.13 min) was obtained followed by the product peaks 4 and 6 during a longer reaction time (1 hr to 2 hr) (Figure 4, Supplemental Figure S3). However, analysis of the products obtained until 30 min showed the highest formation of peak 4 followed by peaks 1 and 6 (Supplemental Figure S3).

In addition, since surrogated redox proteins generally cause low coupling efficiency during the consumption of either substrates or co-factors and thus can generate reactive oxygen

species (ROS), the *in vitro* conversions were performed with the addition of radical scavengers for the ratio of 1: 10: 3 of CYP260A1: Adx: AdR. As scavenging agents ascorbate (neutralizing the superoxide radical, singlet oxygen and hydroxyl radicals), catalase (decomposing hydrogen peroxide to water and oxygen) and superoxide dismutase (SOD) (scavenger of superoxide anion) were employed either individually or in combination. There was no significant decrease in the catalytic rate compared with the control (Figure 5, Supplemental Table S3). In addition, to exclude the role of possible H_2O_2-mediated substrate conversion in the P450 catalysis [35, 42, 59], the *in vitro* conversion of DOC was also performed in the presence of hydrogen peroxide. However, using H_2O_2 only a negligible amount of product was formed.

An *E. coli* based whole cell bioconversion of DOC and characterization of the products

Since we were interested to characterize the product peaks 1, 4 and 6, which were changed according to the availability of the redox proteins in the *in vitro* reaction, CYP260A1 dependent *E. coli* based whole cell bioconversion of DOC was performed. The *in vivo* conversion of DOC using CYP260A1 and a co-expression of Adx and AdR showed an identical product pattern as during the *in vitro* reaction (Figures 6 and 3). Interestingly, the conversion of DOC after 24 hr using resting *E. coli* cells that have been co-expressed with the 3 proteins for 24 hr showed the highest yield of peak 6 (t_R = 7.13 min, $\Delta m/z$ of +2) followed by peak 4 (t_R = 5.28 min, $\Delta m/z$ of +16) and peak 1 (t_R = 7.13 min, $\Delta m/z$ of +32) (Figure 6. A). In contrast, a longer conversion period (48 hr) showed a diminished yield of peak 6 and a subsequent increase of peaks 4 and 1 (Figure 6. B). However, resting cells that were co-expressed with the three proteins for a longer duration (48 hr) showed the highest yield of peak 4 followed by peaks 6 and 1 for both the conversion conditions (24 hr and 48 hr) (Figure 6. C-D). It is interesting that the product peak 1, the yield of which was almost negligible during *in vitro* conversion under steady conditions (performed in the absence of NADPH recycling), has appeared as a major product either during the *in vitro* conversion for a longer time in the presence of NADPH recycling or in the *in vivo* conversion of DOC. Therefore, the appearance of peak 1 seems to be closely related to the availability of sufficient amounts of recycled NADPH and redox proteins.

Our optimized *E. coli* based whole-cell system for the conversion of DOC by CYP260A1 was able to give enough yield to purify the corresponding products. The products comprising the peaks 1, 4 and 6 were purified and characterized by LC-MS and 1D- and 2D-NMR. Products

1 (*Δm/z* of +32), 4 (*Δm/z* of +16) and 6 (*Δm/z* of -2) were identified as 1α-,14α-dihydroxy-11-DOC (1α-,14α-dihydroxylated DOC), 1α-hydroxy-11-DOC (1α-hydroxylated DOC) and 11-deoxycorticosterone-1-ene (21-hydroxypregna-1,4-diene-3, 20-dione or C1-C2-ene-11-DOC), respectively. Product 1 is a novel steroid derivative and the major product 4 is the same one as was identified before as the main product of CYP260A1-dependent DOC conversion [60]. Although CYP260A1 performs mainly the C-1 hydroxylation of DOC, the position at C-2 is prone for hydrogen abstraction and can act as a proton donor. This might result in a chemical modification at C-1 to generate a product with a C-1/C-2 double bond, because of the possible delocalization of the π system after releasing a water molecule from the A-ring. This hypothesis is supported by the existence of the product peak 6 (C1-C2-ene-11-DOC) along with the major peak 4. The NMR data of product 6 also corroborated with the published ^{13}C NMR data [61]. The detailed results of NMR spectroscopy or the products 1, 4 and 6 are as follows.

1α-,14α-dihydroxy-11-deoxycorticosterone (1α-,14α-dihydroxylated DOC) (Product 1): ^{1}H-NMR (500 MHz, $CDCl_3$): d = 0.71 (s, 3H; H-18), 1.12 (m, H-7a), 1.19 (s, 3H, H-19), 1.24 (m, H-12), 1.40 (m, H-15a), 1.59 (m, H-15b), 1.62 (m, H-8), 1.69 (m, H-9), 1.78 (m, H-17), 1.83 (m, H-7b), 2.38 (m, H-6), 2.56 (dd, *J* = 16.9, 3.0, H-2a), 2.68 (m, H-16), 2.75 (dd, *J* = 16.9, 2.5, H-2b), 3.04 (br s, OH-21), 4.09 (s, H-1), 4.30 (d, 19.9, H-21a), 4.65 (d, *J* = 19.9, H-21b), 5.80 ppm (s, H-4); **^{13}C-NMR (125 MHz, $CDCl_3$)**: d = 15.1 (C-18), 18.9 (C-19), 29.2 (C-8), 29.9 (C-12), 31.5 (C-7), 33.2 (C-6), 34.4 (C-16), 43.0 (C-10), 43.1 (C-2), 44.2 (C-9), 48.5 (C-13), 50.6 (C-17), 67.6 (C-21), 72.2 (C-1), 88.9 (C-14), 123.8 (C-4), 166.3 (C-5), 210.0 ppm (C-20).

1α-hydroxy-11-deoxycorticosterone (1α-hydroxylated DOC), (Product 4): ^{1}H-NMR (500 MHz, $CDCl_3$): d = 0.69 (s, 3H; H-18), 1.08 (dddd, J = 13.0, 13.0, 11.5, 5.5, H-7a), 1.18 (s, 3H, H-19), 1.24 (m, H-14), 1.34 (m, H-15a), 1.42 (m, H-12a), 1.43 (m, H-11a), 1.56 (ddd, *J* = 11.5, 11.0, 3.5, H-8), 1.66 (dddd, *J* = 11.5, 11.5, 3.5, 3.5, H-11b), 1.70 (m, H-9), 1.77 (m, H-16a), 1.78 (m, H-15b), 1.83 (m, H-7b), 1.93 (m, H-12b), 2.22 (m, H-16), 2.36 (m, H-6a), 2.39 (m, H-6b), 2.46 (dd, *J* = 9.0, 9.0, H-7b), 2.55 (dd, *J* = 17.0, 3.5, H-2a), 2.75 (dd, *J* = 17.0, 3.0, H-2b), 3.21 (dd, *J* = 4.5, 4.0 OH-21), 4.08 (dd, *J* = 3.5, 3.0, H-1), 4.14 (dd, *J* = 19.0, 4.0, H-21a) 4.20 (dd, *J* = 19.0, 4.5, H-21b), 5.79 ppm (dd, *J* = 1.0, 1.0, H-4); **^{13}C-NMR (125 MHz, $CDCl_3$)**: d = 13.4 (C-18), 18.5 (C-19), 20.3 (C-11), 23.0 (C-16), 24.6 (C-15), 31.0 (C-7), 32.8 (C-6), 35.2 (C-8), 38.2 (C-12), 42.9 (C-2), 43.2 (C-10), 44.7 (C-9), 44.7 (C-13), 56.1 (C-14),

59.1 (C-17), 69.4 (C-21), 72.0 (C-1), 123.5 (C-4), 166.6 (C-5), 196.4 (C-3), 210.1 ppm (C-20).

11-deoxycorticosterone-1-ene (C1-C2-ene-11-DOC) (Product 6): ^{1}H-NMR (500 MHz, $CDCl_3$): d = 0.70 (s, 3H; H-18), 1.06 (m, H-7a), 1.06 (m, H-9), 1.13 (m, H-14), 1.21 (s, 3H, H-19), 1.26 (m, H-11a), 1.34 (m, H-12a), 1.60 (m, H-15a), 1.62 (m, H-8), 1.67 (m, H-11b), 1.75 (m, H-15b), 1.76 (m, H-16a), 1.94 (m, H-12b), 1.95 (m, H-7b), 2.20 (m, H-16b), 2.30 (m, H-6a), 2.40 (m, H-6b), 2.44 (m, H-17), 4.16 (d, *J* = 6.4 Hz, 2H, H-21), 6.06 (t, *J* = 1.5, H-4), 6.23 (dd, *J* = 10.1, 1.8, H-2), 7.02 ppm (d, *J* = 10.1, H-1);**^{13}C-NMR (125 MHz, $CDCl_3$)**: d = 13.6 (C-18), 18.7 (C-19), 22.7 (C-11), 22.9 (C-16), 24.7 (C-15), 32.7 (C-6), 33.5 (C-7), 35.5 (C-8), 38.2 (C-12), 43.4 (C-10), 44.8 (C-13), 52.1 (C-9), 55.6 (C-14), 58.9 (C-17), 69.4 (C-21), 124.0 (C-4), 127.2 (C-2), 155.5 (C-1), 168.8 (C-5), 186.4 (C-3), 210.2 ppm (C-20).

In order to study, whether the product peaks 1 (1α-,14α-dihydroxy-11-DOC) and 6 (C1-C2-ene-11-DOC) were derived from the major product peak 4 (1α-hydroxy-11-DOC), we investigated the conversion of purified 1α-hydroxy-11-DOC either in the presence or absence of a NADPH recycling system with a protein ratio of 1: 10: 3 for CYP260A1: Adx: AdR. We observed the formation of product peaks 1 and 6 during the conversion of 1α-hydroxy-11-DOC thus supporting a processive reaction type. Interestingly, the presence of a NADPH recycling system showed a higher amount of product peak 1 followed by peak 6 compared with the conversion done for 30 min in the absence of the recycling system (Figure 7), suggesting that the availability of higher amounts of redox proteins *in-vitro* promoted the further conversion of the primary product(s) into subsequent secondary product(s). Although we showed further conversion of peak 6 (C1-C2-ene-11-DOC) into peak 4 (1α-hydroxy-11-DOC) under in vivo conditions (Figure 6) or upon complete consumption of DOC in the in vitro reaction (Figure 4, Supplemental Figure S3), it seemed controversial that peak 6 was also observed during the conversion of peak 4 (1α-hydroxy-11-DOC) as a substrate (Figure 7). However, because of the possible delocalization of the π-system during the release of a water molecule from the A-ring of 1α-hydroxy-11-DOC, the C-1 could readily generate isomers with a C-1 and C-2 double bond to give peak 6 (C1-C2-ene-11-DOC). The mechanism for the predominance of peak 4 either by a spontaneous conversion of C1-C2-ene-11-DOC or CYP260A1 mediated hydration reaction is not elucidated.

Since we observed the further conversion of 1α-hydroxy-11-DOC to 1α-,14α-dihydroxy-11-DOC and C1-C2-ene-11-DOC by CYP260A1, we were interested to study the binding affinity of DOC and its major conversion product 1α-hydroxy-11-DOC for CYP260A1. Interestingly, 1α-hydroxy-11-DOC showed an about ~2-fold tighter binding compared with DOC displaying K_d values of 0.52 ± 0.14 µM and 0.27 ± 0.01 µM for DOC and 1α-hydroxy-11-DOC, respectively (Figure 8). This observation suggests that the binding of the surrogate redox partners might have induced an open confirmation of CYP260A1so that 1α-hydroxy-11-DOC can be released from CYP260A1 and enter again into the active site of CYP260A1 in a different orientation. Indeed, our very recent study on the docking of DOC into the crystal structure of CYP260A1 also showed two different orientations of DOC in its active site [59], in which DOC was oriented either having ring-A or ring-D close to the heme-center (Supplementary Figure S4). We hypothesized that the major product 1α-hydroxy-11-DOC might have re-entered into the active site of CYP260A1 in a flipped orientation compared to the position allowing the most feasible 1α-hydroylation to reveal an additional hydroxylation site at position 14 producing 1α,14α-dihydroxy-11-DOC. Most importantly, the observed open conformation of P450cam complexed with its redox partner putidaredoxin (Pdx) in the crystal structure of oxidized and reduced form [62] also suggested that the redox protein induced an open conformation.

In conclusion, the conversion of DOC by CYP260A1 showed three main product peaks (1, 4 and 6) and the product patterns varied in dependence on the employed redox protein ratios. A low concentration of the redox proteins (CYP260A1: Adx: AdR of 1: 5: 3) showed the formation of peak 6 (C1-C2-ene-11-DOC) as the major one followed by peak 4 (P6>P4). When using higher redox protein ratios (1: 10: 3 and 1: 20: 3 for CYP260A1: Adx: AdR), the *in vitro* conversion showed the formation of peak 4 (1α-hydroxy-11-DOC) as the major one. However, the product peak 6 was higher for the ratio 1: 10: 3 compared with 1: 20: 3 showing product patterns of P4>P6>P1 and P4>P1>P6, respectively (Figure 3). In addition, the presence of higher amounts of redox proteins (CYP260A1: Adx: AdR of 1: 20: 3) and the availability of a cofactor (NADPH) recycling system showed the highest yield of the product peak 1 (1α-, 14α-dihydroxy-11-DOC) followed by the peaks 4 and peak 6 (Figure 4). We also showed the conversion of the purified product of peak 4 into peaks 1 and 6, suggesting further conversion of the preformed product(s). Taken together, this study showed that the amount of redox partners can be used to tune the P450-dependent reaction either producing one main product (1α-hydroxy-11-DOC) or getting a more diverse product spectrum (e.g. 1α-, 14α-dihydroxy-11-DOC or C1-C2-ene-11-DOC) as illustrated in Scheme 1.

Acknowledgement

This work was supported by a grant from the BMBF (031A166A). The authors thank Birgit Heider-Lips for protein purification and Dr. Josef Zapp for measuring the NMR samples.

Author contributions

YK and RB designed the concept of the project, analyzed and interpreted the results. YK performed the experiments and wrote the manuscript, and AS contributed to the NMR analysis. We would like to thank Martin Litzenburger for the technical discussion on the NMR analysis.

References

1. Guengerich FP & Munro AW (2013) Unusual cytochrome p450 enzymes and reactions. *J Biol Chem* **288**, 17065-17073.
2. Bernhardt R (2006) Cytochromes P450 as versatile biocatalysts. *J Biotechnol* **124**, 128-145.
3. Podust LM & Sherman DH (2012) Diversity of P450 enzymes in the biosynthesis of natural products. *Nat Prod Rep* **29**, 1251-1266.
4. Hannemann F, Bichet A, Ewen KM & Bernhardt R (2007) Cytochrome P450 systems--biological variations of electron transport chains. *Biochim Biophys Acta* **3**, 330-344.
5. Bernhardt R & Urlacher VB (2014) Cytochromes P450 as promising catalysts for biotechnological application: chances and limitations. *Appl Microbiol Biotechnol* **98**, 6185-6203.
6. McLean KJ, Luciakova D, Belcher J, Tee KL & Munro AW (2015) Biological diversity of cytochrome P450 redox partner systems. *Adv Exp Med Biol* **851**, 299-317.
7. Ewen KM, Schiffler B, Uhlmann-Schiffler H, Bernhardt R & Hannemann F (2008) The endogenous adrenodoxin reductase-like flavoprotein arh1 supports heterologous cytochrome P450-dependent substrate conversions in Schizosaccharomyces pombe. *FEMS Yeast Res* **8**, 432-441.
8. Jenkins CM & Waterman MR (1998) NADPH−Flavodoxin Reductase and Flavodoxin from Escherichia coli: Characteristics as a Soluble Microsomal P450 Reductase. *Biochemistry* **37**, 6106-6113, doi: 10.1021/bi973076p.

9. Girhard M, Klaus T, Khatri Y, Bernhardt R & Urlacher VB (2010) Characterization of the versatile monooxygenase CYP109B1 from Bacillus subtilis. *Appl Microbiol Biotechnol* **87**, 595-607.
10. Khatri Y, Ringle M, Lisurek M, von Kries JP, Zapp J & Bernhardt R (2016) Substrate Hunting for the Myxobacterial CYP260A1 Revealed New 1alpha-Hydroxylated Products from C-19 Steroids. *Chembiochem* **17**, 90-101.
11. Girhard M, Schuster S, Dietrich M, Dürre P & Urlacher VB (2007) Cytochrome P450 monooxygenase from Clostridium acetobutylicum: A new α-fatty acid hydroxylase. *Biochem Biophys Res Commun* **362**, 114-119.
12. Roberts GA, Celik A, Hunter DJ, Ost TW, White JH, Chapman SK, Turner NJ & Flitsch SL (2003) A self-sufficient cytochrome p450 with a primary structural organization that includes a flavin domain and a [2Fe-2S] redox center. *J Biol Chem* **278**, 48914-48920.
13. Zhang A, Zhang T, Hall EA, Hutchinson S, Cryle MJ, Wong LL, Zhou W & Bell SG (2015) The crystal structure of the versatile cytochrome P450 enzyme CYP109B1 from Bacillus subtilis. *Mol Biosyst* **11**, 869-881.
14. Kern F, Dier TK, Khatri Y, Ewen KM, Jacquot JP, Volmer DA & Bernhardt R (2015) Highly Efficient CYP167A1 (EpoK) dependent Epothilone B Formation and Production of 7-Ketone Epothilone D as a New Epothilone Derivative. *Sci Rep* **5**, 14881.
15. Ringle M, Khatri Y, Zapp J, Hannemann F & Bernhardt R (2013) Application of a new versatile electron transfer system for cytochrome P450-based Escherichia coli whole-cell bioconversions. *Appl Microbiol Biotechnol* **97**, 7741-7754.
16. Aliverti A, Jansen T, Zanetti G, Ronchi S, Herrmann RG & Curti B (1990) Expression in Escherichia coli of ferredoxin:NADP+ reductase from spinach. Bacterial synthesis of the holoflavoprotein and of an active enzyme form lacking the first 28 amino acid residues of the sequence. *Eur J Biochem* **191**, 551-555.
17. Piubelli L, Aliverti A, Bellintani F & Zanetti G (1995) Spinach ferredoxin i: overproduction in Escherichia coli and purification. *Protein Expr Purif* **6**, 298-304.
18. Khatri Y, Girhard M, Romankiewicz A, Ringle M, Hannemann F, Urlacher VB, Hutter MC & Bernhardt R (2010) Regioselective hydroxylation of norisoprenoids by CYP109D1 from Sorangium cellulosum So ce56. *Appl Microbiol Biotechnol* **88**, 485-495.
19. Khatri Y, Hannemann F, Girhard M, Kappl R, Meme A, Ringle M, Janocha S, Leize-Wagner E, Urlacher VB & Bernhardt R (2013) Novel family members of CYP109 from

Sorangium cellulosum So ce56 exhibit characteristic biochemical and biophysical properties. *Biotechnol Appl Biochem* **60**, 18-29.

20. Khatri Y, Hannemann F, Girhard M, Kappl R, Hutter M, Urlacher VB & Bernhardt R (2015) A natural heme-signature variant of CYP267A1 from Sorangium cellulosum So ce56 executes diverse omega-hydroxylation. *FEBS J* **282**, 74-88.
21. Schiffer L, Brixius-Anderko S, Hannemann F, Zapp J, Neunzig J, Thevis M & Bernhardt R (2016) Metabolism of Oral Turinabol by Human Steroid Hormone-Synthesizing Cytochrome P450 Enzymes. *Drug Metab Dispos* **44**, 227-237.
22. Koo LS, Immoos CE, Cohen MS, Farmer PJ & Ortiz de Montellano PR (2002) Enhanced Electron Transfer and Lauric Acid Hydroxylation by Site-Directed Mutagenesis of CYP119. *J Am Chem Soc* **124**, 5684-5691.
23. Bellamine A, Mangla AT, Nes WD & Waterman MR (1999) Characterization and catalytic properties of the sterol 14alpha-demethylase from Mycobacterium tuberculosis. *Proc Natl Acad Sci U S A* **96**, 8937-8942.
24. Cryle MJ, Ortiz de Montellano PR & De Voss JJ (2005) Cyclopropyl Containing Fatty Acids as Mechanistic Probes for Cytochromes P450. *J Org Chem* **70**, 2455-2469.
25. Ewen KM, Hannemann F, Khatri Y, Perlova O, Kappl R, Krug D, Huttermann J, Muller R & Bernhardt R (2009) Genome mining in Sorangium cellulosum So ce56: identification and characterization of the homologous electron transfer proteins of a myxobacterial cytochrome P450. *J Biol Chem* **284**, 28590-28598.
26. Tang EK, Tieu EW & Tuckey RC (2012) Expression of human CYP27B1 in Escherichia coli and characterization in phospholipid vesicles. *FEBS J* **279**, 3749-3761.
27. Bell SG, Spence JTJ, Liu S, George JH & Wong L-L (2014) Selective aliphatic carbon-hydrogen bond activation of protected alcohol substrates by cytochrome P450 enzymes. *Org Biomol Chem* **12**, 2479-2488.
28. Girhard M, Klaus T, Khatri Y, Bernhardt R & Urlacher VB (2010) Characterization of the versatile monooxygenase CYP109B1 from Bacillus subtilis. *Appl Microbiol Biotechnol* **87**, 595-607.
29. Milhim M, Gerber A, Neunzig J, Hannemann F & Bernhardt R (2016) A Novel NADPH-dependent flavoprotein reductase from Bacillus megaterium acts as an efficient cytochrome P450 reductase. *J Biotechnol* **231**, 83-94.
30. Khatri Y, Hannemann F, Ewen KM, Pistorius D, Perlova O, Kagawa N, Brachmann AO, Muller R & Bernhardt R (2010) The CYPome of Sorangium cellulosum So ce56

and identification of CYP109D1 as a new fatty acid hydroxylase. *Chem Biol* **17**, 1295-1305.

31. Zhang W, Liu Y, Yan J, Cao S, Bai F, Yang Y, Huang S, Yao L, Anzai Y, Kato F, et al. (2014) New reactions and products resulting from alternative interactions between the P450 enzyme and redox partners. *J Am Chem Soc* **136**, 3640-3646.
32. Schifrin A, Khatri Y, Kirsch P, Thiel V, Schulz S & Bernhardt R (2016) A single terpene synthase is responsible for a wide variety of sesquiterpenes in Sorangium cellulosum Soce56. *Org Biomol Chem* **14**, 3385-3393.
33. Guengerich FP, Sohl CD & Chowdhury G (2011) Multi-step oxidations catalyzed by cytochrome P450 enzymes: Processive vs. distributive kinetics and the issue of carbonyl oxidation in chemical mechanisms. *Arch Biochem Biophys* **507**, 126-134.
34. Sohl CD & Guengerich FP (2010) Kinetic analysis of the three-step steroid aromatase reaction of human cytochrome P450 19A1. *J Biol Chem* **285**, 17734-17743.
35. Khatri Y, Luthra A, Duggal R & Sligar SG (2014) Kinetic solvent isotope effect in steady-state turnover by CYP19A1 suggests involvement of Compound 1 for both hydroxylation and aromatization steps. *FEBS Lett* **588**, 3117-3122.
36. Chowdhury G, Calcutt MW & Peter Guengerich F (2010) Oxidation of N-nitrosoalkylamines by human cytochrome p450 2a6: Sequential oxidation to aldehydes and carboxylic acids and analysis of reaction steps. *J Biol Chem* **285**, 8031-8044.
37. Nguyen KT, Virus C, Gunnewich N, Hannemann F & Bernhardt R (2012) Changing the regioselectivity of a P450 from C15 to C11 hydroxylation of progesterone. *Chembiochem* **13**, 1161-1166.
38. Sagara Y, Wada A, Takata Y, Waterman MR, Sekimizu K & Horiuchi T (1993) Direct expression of adrenodoxin reductase in *Escherichia coli* and the functional characterization. *Biol Pharm Bul.* **16**, 627-630.
39. Uhlmann H, Kraft R & Bernhardt R (1994) C-terminal region of adrenodoxin affects its structural integrity and determines differences in its electron transfer function to cytochrome P-450. *J Biol Chem* **269**, 22557-22564.
40. Williams JW & Morrison JF (1979) The kinetics of reversible tight-binding inhibition. *Methods Enzymol* **63**, 437-467.
41. Kern F, Khatri Y, Litzenburger M & Bernhardt R (2016) CYP267A1 and CYP267B1 from Sorangium cellulosum So ce56 are Highly Versatile Drug Metabolizers. *Drug Metab Dispos* **44**, 495-504.

42. Kiss FM, Khatri Y, Zapp J & Bernhardt R (2015) Identification of new substrates for the CYP106A1-mediated 11-oxidation and investigation of the reaction mechanism. *FEBS Lett* **589**, 2320-2326.
43. Salamanca-Pinzon SG, Khatri Y, Carius Y, Keller L, Muller R, Lancaster CR & Bernhardt R (2016) Structure-function analysis for the hydroxylation of Delta4 C21-steroids by the myxobacterial CYP260B1. *FEBS Lett* **590**, 1838-51.
44. Ewen KM, Ringle M & Bernhardt R (2012) Adrenodoxin - a versatile ferredoxin. *IUBMB Life* **64**, 506-512.
45. Ewen KM, Kleser M & Bernhardt R (2011) Adrenodoxin: the archetype of vertebrate-type [2Fe-2S] cluster ferredoxins. *Biochim Biophys Acta* **1814**, 111-125.
46. Chun Y-J, Shimada T, Sanchez-Ponce R, Martin MV, Lei L, Zhao B, Kelly SL, Waterman MR, Lamb DC & Guengerich FP (2007) Electron transport pathway for a streptomyces cytochrome p450: cytochrome P450 105D5-catalyzed fatty acid hydroxylation in streptomyces coelicolor a3(2). *J Biol Chem.* **282**, 17486-17500.
47. Xiang H, Tschirret-Guth RA & Ortiz de Montellano PR (2000) An A245T Mutation Conveys on Cytochrome P450eryF the Ability to Oxidize Alternative Substrates. *J Biol Chem* **275**, 35999-36006.
48. Hanukoglu I & Hanukoglu Z (1986) Stoichiometry of mitochondrial cytochromes P-450, adrenodoxin and adrenodoxin reductase in adrenal cortex and corpus luteum. Implications for membrane organization and gene regulation. *Eur J Biochem* **157**, 27-31.
49. Meharenna YT, Slessor KE, Cavaignac SM, Poulos TL & De Voss JJ (2008) The critical role of substrate-protein hydrogen bonding in the control of regioselective hydroxylation in p450cin. *J Biol Chem* **283**, 10804-10812.
50. Anzai Y, Li S, Chaulagain MR, Kinoshita K, Kato F, Montgomery J & Sherman DH (2008) Functional Analysis of MycCI and MycG, Cytochrome P450 Enzymes Involved in Biosynthesis of Mycinamicin Macrolide Antibiotics. *Chem Biol* **15**, 950-959.
51. Sherman DH, Li S, Yermalitskaya LV, Kim Y, Smith JA, Waterman MR & Podust LM (2006) The Structural Basis for Substrate Anchoring, Active Site Selectivity, and Product Formation by P450 PikC from Streptomyces venezuelae. *J Biol Chem.* **281**, 26289-26297.
52. Frank DJ, Zhao Y, Wong SH, Basudhar D, De Voss JJ & Ortiz de Montellano PR (2016) Cholesterol Analogs with Degradation-resistant Alkyl Side Chains Are Effective Mycobacterium tuberculosis Growth Inhibitors. *J Biol Chem* **291**, 7325-7333.

53. Tuckey RC & Cameron KJ (1993) Catalytic properties of cytochrome P-450scc purified from the human placenta: comparison to bovine cytochrome P-450scc. *Biochim Biophys Acta* **13**, 185-194.
54. Tuckey RC & Sadleir J (1999) The concentration of adrenodoxin reductase limits cytochrome p450scc activity in the human placenta. *Eur J Biochem* **263**, 319-325.
55. Pikuleva IA, Tesh K, Waterman MR & Kim Y (2000) The tertiary structure of full-length bovine adrenodoxin suggests functional dimers. *Arch Biochem Biophys* **373**, 44-55.
56. Faro M, Schiffler B, Heinz A, Nogues I, Medina M, Bernhardt R & Gomez-Moreno C (2003) Insights into the design of a hybrid system between Anabaena ferredoxin-NADP+ reductase and bovine adrenodoxin. *Eur J Biochem* **270**, 726-735.
57. Behlke J, Ristau O, Muller EC, Hannemann F & Bernhardt R (2007) Self-association of adrenodoxin studied by using analytical ultracentrifugation. *Biophys Chem* **125**, 159-165.
58. Hannemann F, Guyot A, Zollner A, Muller JJ, Heinemann U & Bernhardt R (2009) The dipole moment of the electron carrier adrenodoxin is not critical for redox partner interaction and electron transfer. *J Inorg Biochem* **103**, 997-1004.
59. Khatri Y, Gregory MC, Grinkova YV, Denisov IG & Sligar SG (2014) Active site proton delivery and the lyase activity of human CYP17A1. *Biochem Biophys Res Commun* **443**, 179-184.
60. Carius Y, Ringle M, Lancaster CR, & Bernhardt R. (2016) Structural characterization of CYP260A1 from Sorangium cellulosum to investigate the 1alpha-hydroxylation of a mineralocorticoid. *FEBS Lett* 590, 4638-4648.
61. Gonzalez MD & Burton G (1984) A carbon-13 nuclear magnetic resonance study of the 1,4-diene analogues of steroid hormones and related steroids. O*rg Magn Resonance* **22**, 586-591.
62. Tripathi S, Li H & Poulos TL (2013) Structural basis for effector control and redox partner recognition in cytochrome P450. *Science* **340**, 1227-1230.

Figure legends

Figure 1: Steady-state conversion of DOC by CYP260A1. A. Chromatogram showing the conversion of DOC. The activity was reconstituted with the heterologous redox partners Adx

and AdR. The ratio of CYP260A1: Adx: AdR was 1: 10: 3 containing 0.5 µM of CYP260A1 in a 250 µl reaction mixture. The reaction was started with the addition of NADPH (500 µM) in the absence of cofactor regeneration. The numbers indicated in the chromatogram represent the product peaks for the conversion of DOC. The peak 'S' represents the substrate DOC. The products corresponding to peaks 1, 4 and 6 were identified as 1α-, 14α-dihydroxy-11-DOC, 1α-hydroxy-11-DOC, and 11-deoxycorticosterone-1-ene (C1-C2-ene-11-DOC), respectively. B. Time dependent (0-100 min) conversion of DOC. C. NADPH dependent conversion of DOC by CYP260A1. Different concentrations of NADPH (0–4 mM) were used. V_{max} and K_m values were determined by plotting the substrate conversion velocities versus the corresponding NADPH concentrations and subsequently using a hyperbolic fit (SIGMAPLOT software). D. Steady-state conversion of DOC in the presence (+, solid bar) and absence (-, empty bar) of cofactor (NADPH) regeneration (recycling), as explained in the 'material and methods' section. The number on the bar represents the value of the activity. The error bar in the figures represents the standard deviation of 3–5 independent measurements.

Figure 2: Steady-state conversion of DOC using different ratios of CYP260A1, Adx and AdR. Different concentrations of CYP260A1 and the redox partners Adx and AdR are shown in the Y-axis and the X-axis represents the activity (nmol total product per nmol CYP260A1 per min). The value inside the bar represents the ratio of CYP260A1: Adx: AdR with respect to the concentrations as shown in the Y-axis. The entries A-E (light brown) represent the ratio of CYP260A1: Adx: AdR of 1: 1: 1, 1: 2: 0.5, 1: 1: 5, 3: 2.5: 1, 8: 3: 1, respectively. These ratios were used for the *in vitro* conversion in other studies. The entries F-H (blue bars), I-N (green bars) and O-U (yellow bars) represent the redox protein pool consisting of 5-, 10- and 20-folds higher Adx concentration compared with CYP260A1 in the *in vitro* conversion of DOC, in which the AdR ratio is increased as indicated. The number on the bar represents the value of the activity. The error bar represents the standard deviation of 3 independent measurements. All the reactions were started adding NADPH (500 µM) and incubated for 20 min in the absence of a NADPH recycling system. The same batches of the purified proteins were used for the reaction.

Figure 3: Comparison of the HPLC chromatogram traces obtained for the DOC conversion using different ratios of CYP260A1 and the redox partners *in vitro* (Panel I). The chromatogram of DOC alone (A) represented by peak S, and *in vitro* product patterns in the

absence of a NADPH recycling system (B-D) using ratios of CYP260A1: Adx: AdR of 1: 5: 3 (B), 1: 10: 3 (C) and 1: 20: 3 (D) are shown. The numbers indicated in the chromatogram represent the product peaks for the conversion of DOC. The products corresponding to peaks 1, 4 and 6 were identified as 1α-, 14 α-dihydroxy-11-DOC, 1α-hydroxy-11-DOC, and C1-C2-ene-11-DOC, respectively. Bar diagram showing the comparison of the major products obtained from the *in vitro* conversion of DOC by CYP260A1 in the absence of a NADPH recycling system (Panel II). The relative percentage of the product peaks 1 (black bar), 4 (gray bar) and 6 (empty bar) of the DOC conversion are shown. The number on the bar represents the value of the relative selectivity (in %) for the products. The error bar represents the standard deviation of 3-5 independent measurements, and the values are shown in Supplemental Table S1.

Figure 4: A. Chromatogram showing the *in vitro* conversion of DOC by CYP260A1. The reaction mixture consists of CYP260A1: Adx: AdR of 1: 20: 3 in the presence of a NADPH recycling system. The conversion was done for 1 hr. The products corresponding to peaks 1, 4 and 6 were identified as 1α-, 14 α-dihydroxy-11-DOC, 1α-hydroxy-11-DOC, and C1-C2-ene-11-DOC, respectively. The peak 'S' represents the substrate DOC. B. The relative percentage of the product peaks 1 (black bar), 4 (gray bar) and 6 (empty bar) of DOC conversion are shown. The number on the bar represents the value of the relative selectivity (in %) for the products. The error bar represents the standard deviation of 3-5 independent measurements, and the values are shown in the Supplemental Table S2.

Figure 5: The effect of radical scavengers on the catalytic rate of DOC conversion by CYP260A1. The error bars represent the standard deviation of 3 independent measurements, and the values are shown in the Supplemental Table S3. *SOD, superoxide dismutase.

Figure 6: The *E. coli* based whole-cell conversion of DOC by CYP260A1. The product pattern of DOC conversion obtained after 24 hr (A) and 48 hr (B) by co-expressing CYP260A1, Adx and AdR for 24 hr in the *E. coli* cells was compared with the conversion of the substrate for 24 hr (C) and 48 hr (D) using 48 hr co-expressed cells (Panel I). The numbers indicated in the chromatogram represent the percentage of the product peaks for the conversion of DOC. The products corresponding to peaks 1, 4 and 6 were identified as 1α-, 14α-dihydroxy-11-DOC, 1α-hydroxy-11-DOC, and C1-C2-ene-11-DOC, respectively. The

peak ‘S’ represents the substrate DOC. The relative percentage of the product peaks 1 (black bar), 4 (gray bar) and 6 (empty bar) of DOC conversion are shown (Panel II). The number on the bar represents the value of the relative percentage selectivity for the products. The error bar represents the standard deviation of 3-5 independent measurements, and the values are shown in the Supplemental Table S4.

Figure 7: Conversion of 1α-hydroxy-11-DOC by CYP260A1. Chromatograms of DOC (A) and the purified 1α-hydroxy-11-DOC (B); the chromatogram showing the conversion of 1α-hydroxy-11-DOC, peak 4, (B) into the product peaks 1 and 6 in the absence (C) and presence (D) of a NADPH recycling system. The activity was reconstituted with the heterologous redox partners Adx and AdR. The ratio of CYP260A1: Adx: AdR was 1: 10: 3. The reactions in the absence (C) and presence (D) of a NADPH recycling system were done for 30 min and 1hr respectively. The products corresponding to peaks 1, 4 and 6 were identified as 1α-, 14α-dihydroxylated-11-DOC, 1α-hydroxy-11-DOC, and 11-deoxycorticosterone-1-ene (C1-C2-ene-11-DOC), respectively. The asterisk ‘*’ represent the unidentified product.

Figure 8: DOC (Panel I) and 1α-hydroxy-11-DOC (Panel II) binding to CYP260A1. The absorbance spectra of oxidized CYP260A1 (1.12 μM, panel I, and 0.90 μM, panel II) and increasing concentrations of the substrates are shown in the main image (A), in which the Soret band maximum is gradually shifting from 417 nm (pointing down) to 393 nm (pointing up) during the addition of increasing concentrations of substrates. The inset B shows the overlaid difference spectra produced by subtraction of the spectrum for ligand-free CYP260A1 from the successive spectra for substrate-bound species accumulated during the titration between 0 and 2 μM of DOC (Panel I) and 0 and 2.5 μM of 1α-hydroxy-11-DOC (Panel II). The plots of absorbance change vs. concentration of the substrate from the titration were plotted to a tight binding quadratic equation as described in ‘Materials and Methods’ and the CYP260A1 dissociation constants (K_d value) were identified (inset C).

Scheme 1: Schematic illustration of the effect of redox protein ratios on the product pattern of the DOC (green sphere) conversion by CYP260A1 (red oval). The substrate, DOC (green sphere), is converted into the products 1 (P1, blue sphere), 4 (P4, yellow sphere) and 6 (P6, pink sphere). The products are highlighted by differently colored spheres. At low concentrations of redox proteins (CYP260A1: Adx: AdR of 1: 5: 3) (Path I) the major product 6 (C1-C2-ene-11-DOC) (pink sphere) followed by product 4 (1α-hydroxy-11-DOC) (yellow

sphere) (P6>P4) is shown. Product 1 (blue sphere) was absent in this *in vitro* reaction. The presence of higher (Path II) and excessive (Path III) ratios of the redox proteins showed the formation of product 1 (1α, 14α-dihydroxy-11-DOC) (blue sphere) besides 4 and 6. The redox ratio of 1: 10: 3 for CYP260A1: Adx: AdR showed the formation of product 4 (yellow sphere) as a main product followed by products 6 (pink sphere) and 1 (blue sphere) (P4>P6>P1), whereas the ratio of 1: 20: 3 showed the highest yield of product 4 followed by the products 1 and 6 (P4>P1>P6). The presence of high amounts of redox proteins (CYP260A1: Adx: AdR of 1: 20: 3) and the concomitant availability of a NADPH recycling system showed the highest yield of product peak 1 (1α-, 14α-dihydroxy-11-DOC) (blue sphere) followed by products 4 and 6.

Tables

Table 1: Rate of conversion of DOC by CYP260A1 using different redox protein ratios of Adx and AdR.

CYP260A1: Adx : AdR		Rate (min^{-1})	Remarks
Protein concentation [µM]	**Ratio**	**nmol total products per nmol CYP260A1 per min**	**Figure 2, entry**
0.5: 2.5: 0.5	1: 5: 1	1.10	F
0.5: 2.5: 1.5	1: 5: 3	1.62	G
0.5: 2.5: 2.5	1: 5: 5	0.30 ± 0.06	H
0.5: 5: 0.5	1: 10: 1	1.50 ± 0.12	I
0.5: 5: 1.0	1: 10: 2	1.55 ± 0.02	J
0.5: 5: 1.5	1: 10: 3	1.96 ± 0.10	K
0.5: 5: 2.5	1: 10. 5	0.70	L
0.5: 5: 3.5	1: 10: 7	0.40 ± 0.04	M
0.5: 5: 5.0	1: 10: 10	0.27	N
0.5: 10: 0.5	1: 20: 1	2.36 ± 0.07	O
0.5: 10: 1.5	1: 20: 3	2.61 ± 0.10	P
0.5: 10: 2.5	1: 20: 5	2.44 ± 0.01	Q
0.5: 10: 3.5	1: 20: 7	2.02	R
0.5: 10: 5.0	1: 20: 10	2.18	S
0.5: 10: 7.5	1: 20: 15	1.90	T
0.5: 10: 10.0	1: 20: 20	0.54	U

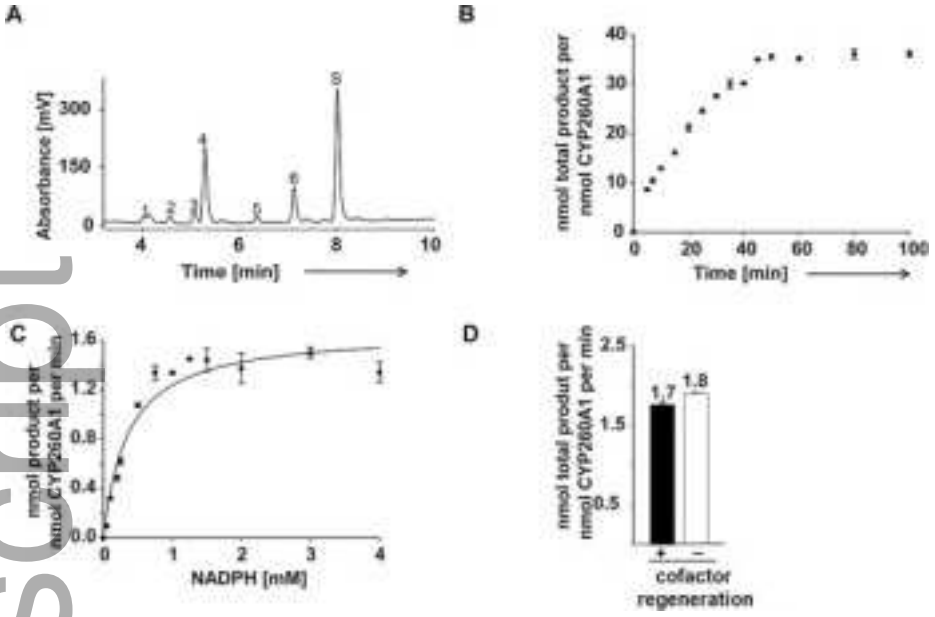

feb2_12619_f1.tif

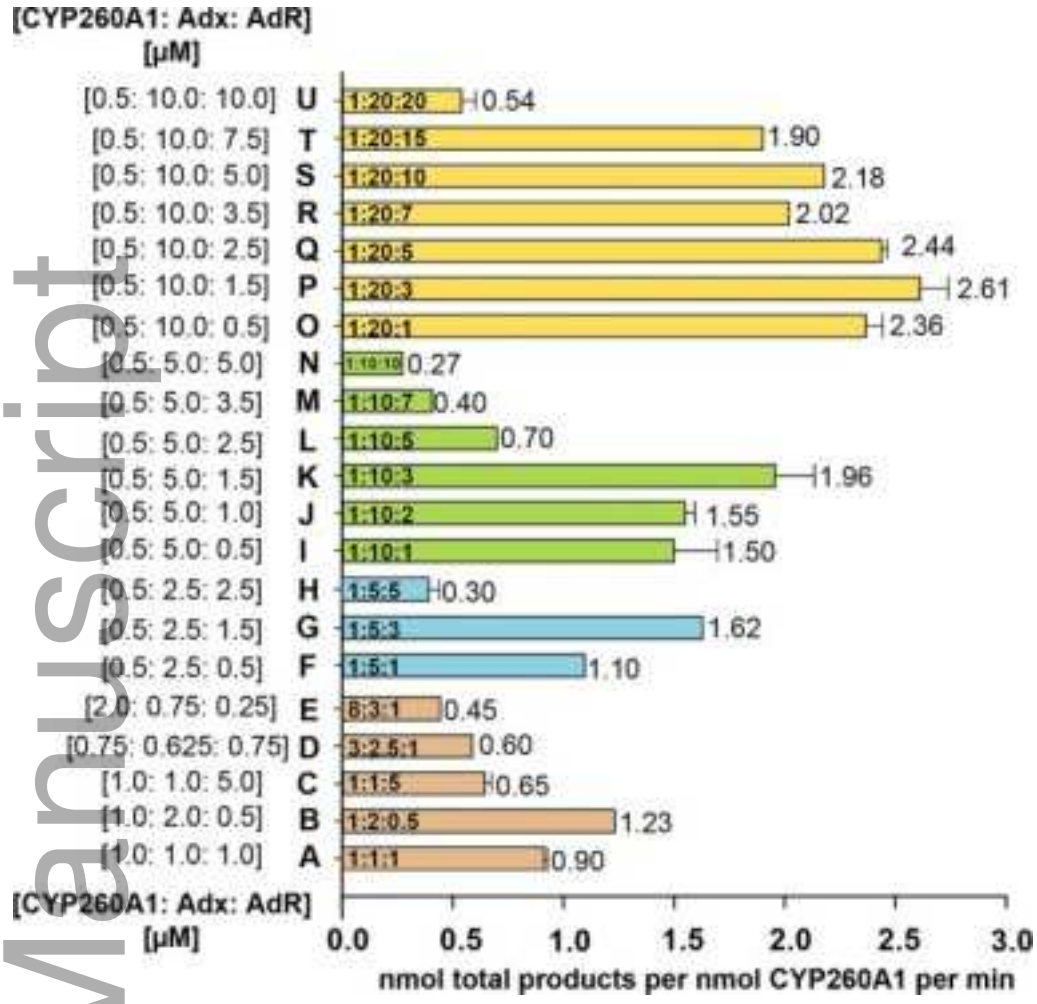

feb2_12619_f2.tif

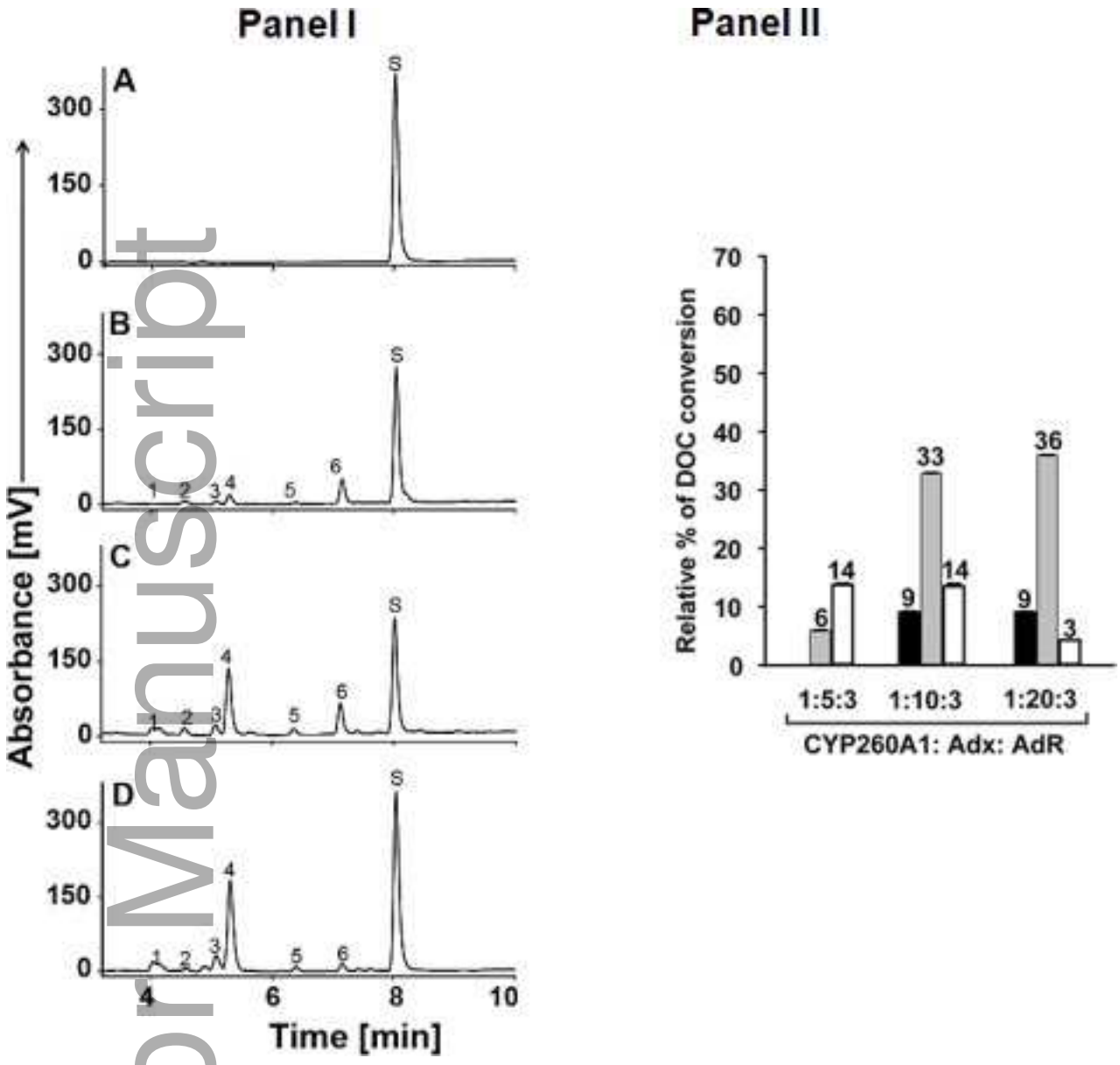

feb2_12619_f3.tif

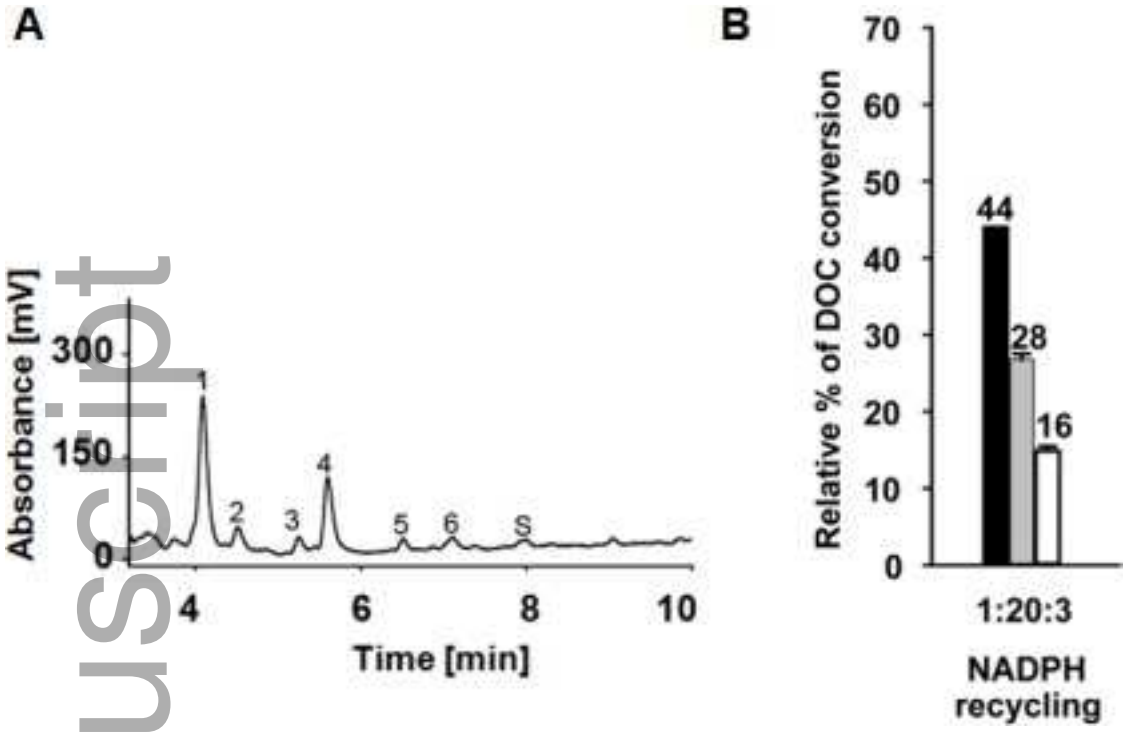

feb2_12619_f4.tif

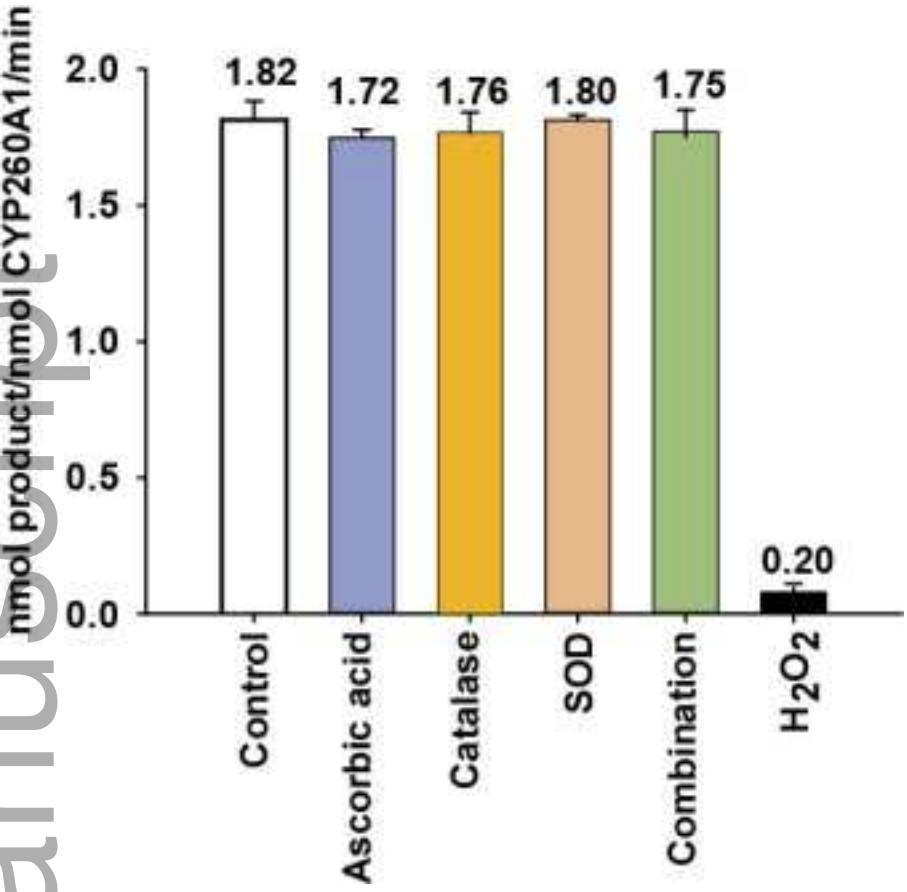

feb2_12619_f5.tif

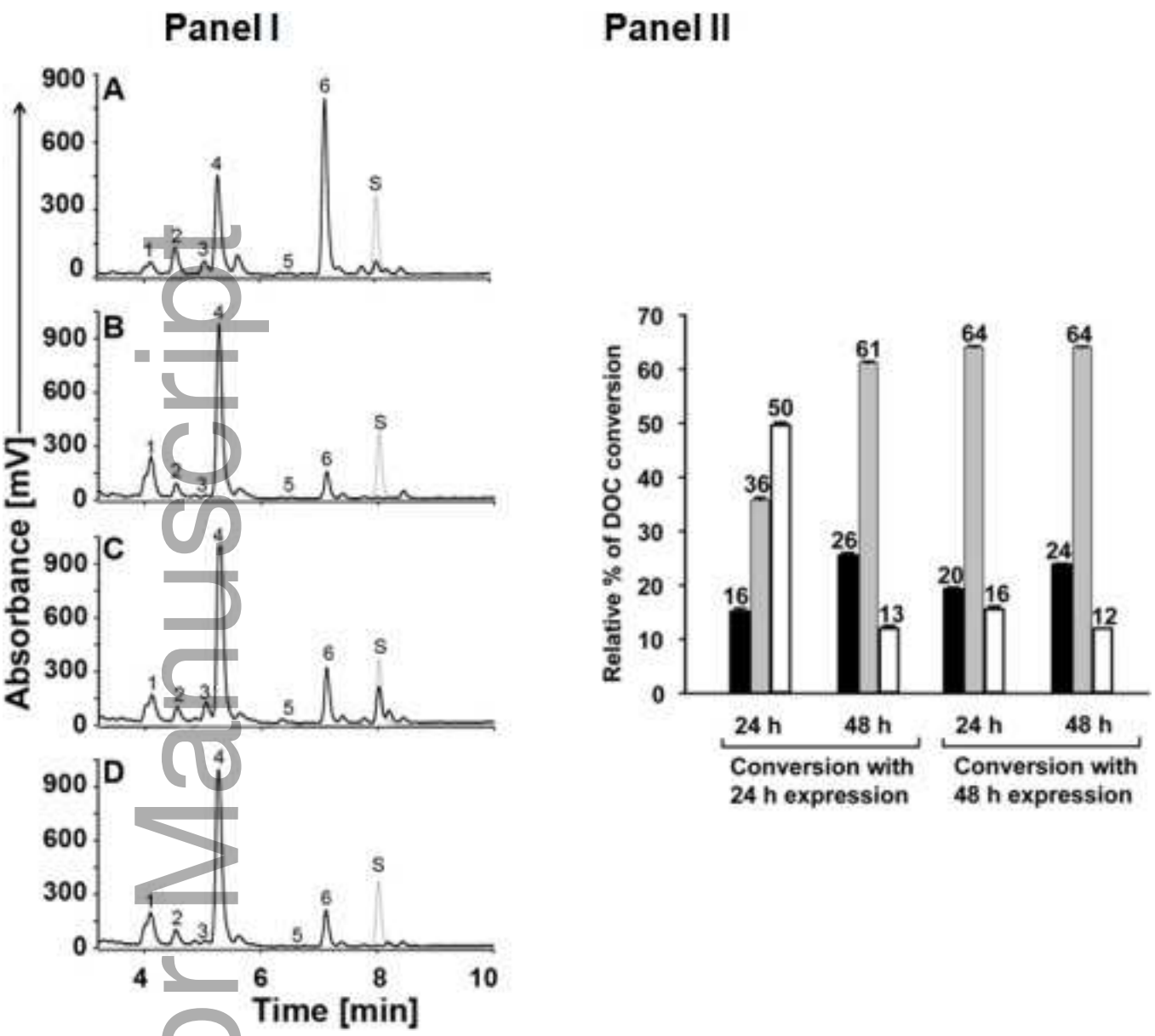

feb2_12619_f6.tif

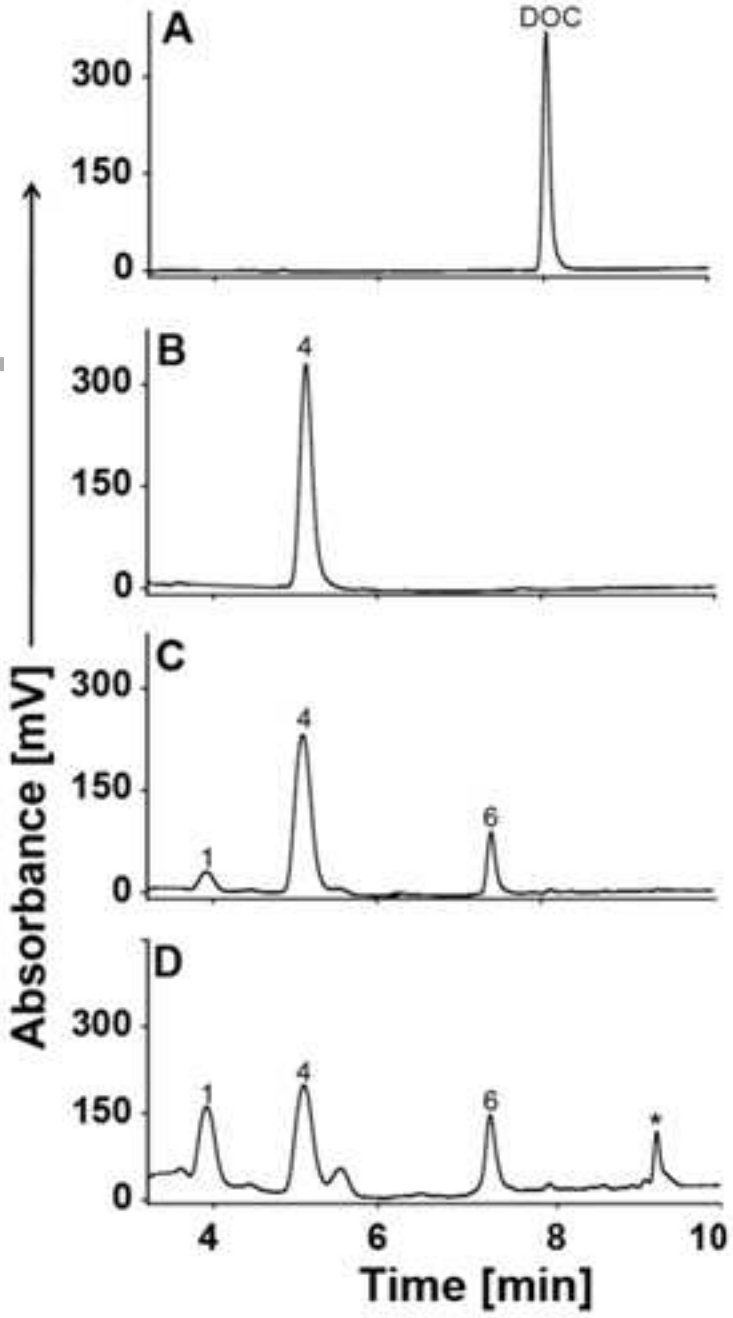

feb2_12619_f7.tif

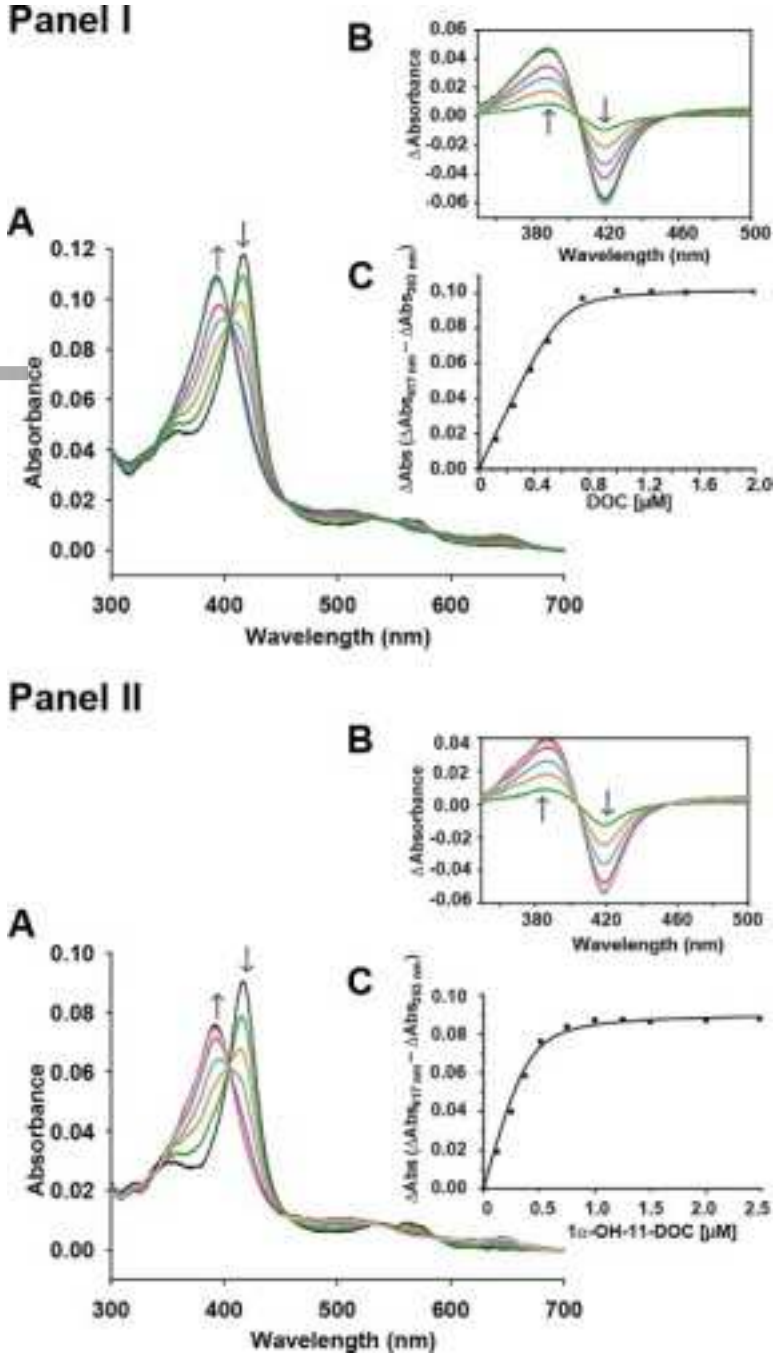

feb2_12619_f8.tif